CHAPTER

# 4.7.1

# Metal sources and sinks

*Leslie J. Robbins*[1], *Kaarel Mänd*[2], *Zhiquan Li*[1,3] *and Kurt O. Konhauser*[3]

[1]Department of Geology, University of Regina, Regina, SK, Canada [2]Department of Geology, University of Tartu, Tartu, Estonia [3]Department of Earth & Atmospheric Sciences, University of Alberta, Edmonton, AL, Canada

## Introduction

As Earth Scientists, we typically view Earth's history through the lens of uniformitarianism, where the present is the key to the past. Doing so provides a useful framework for interpreting geologic evidence. To this end, our understanding of elemental cycling, particularly for trace metals, through time is interpreted in the context of modern environments. Earth's Archean oceans differed significantly from the modern open oceans. From a geochemical perspective, the early oceans had more in common with modern ferruginous lakes, oxygen minimum zones, and restricted anoxic to euxinic (anoxic and sulfide-rich) basins such as the Black Sea or the Cariaco Basin. As discussed in earlier chapters, these differences are specifically manifested in both the iron and sulfur cycles of the Archean oceans, but also those of trace metals.

The Archean Earth surface was characterized by higher atmospheric carbon dioxide ($pCO_2$) (e.g., Krissansen-Totton et al., 2018; Catling and Zahnle, 2020), depressed and, possibly transient, oxygen ($O_2$) levels below $10^{-6}$ times present atmospheric levels (PAL) (Catling and Zahnle, 2020), and limited continental emergence prior to 3.0 Ga (e.g., Hawkesworth et al., 2017; Johnson and Wing, 2020). This resulted in ferruginous (anoxic and iron-rich) marine conditions being the prevailing state for much of Earth's history (Planavsky et al., 2011; Poulton and Canfield, 2011), with euxinic environments largely restricted to continental margins (e.g., Kendall et al., 2010, 2011). Another manifestation of the differences between the anoxic Archean and oxygenated modern environments was changes in the sources and sinks of trace metals. These differences are perhaps most prevalent in redox-sensitive elements (RSEs), which are a group of trace metals whose geochemical cycling depends strongly on the prevailing redox conditions at Earth's surface and in marine settings. The RSE include metals which will be discussed here, such as chromium (Cr), uranium (U), molybdenum (Mo) (Figs. 2 and 3), as well as cobalt (Co) and copper (Cu) (Fig. 4.7.1.4). While not discussed here, vanadium (V) is also an RSE, with a similar conservative behavior in seawater as U and Mo (e.g., Tribovillard et al., 2006). Vanadium is also minimally sourced in riverine detrital material. In addition, the trace metals nickel (Ni) and zinc (Zn) will also be discussed (Fig. 4.7.1.4). We note that a number of the metals discussed here—Mo, Co, Cu, Ni, and Zn, as well as V—have biological uses, such as incorporation into metalloenzymes (see Robbins et al., 2016). While the protracted oxygenation of Earth's surface environments has greatly impacted the cycling and sequestration of metals in marine systems, the discussion here will primarily be constrained to the Archean to early Paleoproterozoic (~4–2.0 billion years ago (Ga)).

The deposition of banded and granular iron formations, collectively referred to here as iron formations (IFs), is an example of how differences in Earth's surface conditions with regards to sources and sinks are manifested in the Archean (Fig. 4.7.1.1). Anoxic conditions on the early Earth, coupled with higher emissions of submarine volcanic ferrous iron ($Fe^{2+}$), allowed for the transport and build-up of appreciable dissolved $Fe^{2+}$ concentrations that led to the conditions required for the deposition of IFs (Bekker et al., 2014; Konhauser et al., 2017). Subsequently, the pool of surface water $Fe^{2+}$ was oxidized by either anoxygenic photoferrotrophs (e.g., Konhauser et al., 2002; Kappler et al., 2005) or free $O_2$ produced by cyanobacteria (e.g., Cloud, 1973; Li et al., 2021). The oxidation of $Fe^{2+}$, either biotically or abiotically, led to the generation and precipitation of ferric (oxy)hydroxides, the primary iron precipitates in


https://doi.org/10.1016/B978-0-323-95547-8.00027-6

FIGURE 4.7.1.1 An outcrop of the 3.22-billion-year-old Moodies group iron formation in South Africa, composed of alternating bands of iron oxide and chert, highlighting the fundamentally different nature of ancient seawater that precipitated this chemical sediment. The field hammer is ~35 cm from top to bottom. *Photo credit: L. Robbins.*

IFs. The operation of an oxidative pathway for $Fe^{2+}$ during IF deposition is well documented, dating back to at least ~3.0 Ga (e.g., Smith et al., 2017, 2020), and perhaps even earlier (Czaja et al., 2013) based on the fractionation of iron isotopes in IF from the 3.77 Ga Isua Supracrustal Belt in Greenland. While the precipitation of ferric (oxy) hydroxides has made IFs a valuable proxy for reconstructing paleoenvironmental conditions (e.g., Bau and Möller, 1993; Robbins et al., 2016; Mänd et al., 2021), several recent studies have challenged the origins of IFs as a sink for oxidized iron, instead linking their deposition to the formation of ferrous silicates within the water column (e.g., Muhling and Rasmussen, 2020; Rasmussen et al., 2021). While IFs serve as an excellent example of how metal cycling differed in the Archean, the remainder of the discussion will be focused on transition metals.

Reconstructing the cycles of various trace metals in the Archean to early Paleoproterozoic has relied upon both thermodynamic approaches (e.g., Anbar and Knoll, 2002; Saito et al., 2003; Anbar; 2008) as well as reconstructions from sedimentary proxies including IFs, shales, carbonates, and sedimentary to early diagenetic pyrites (see Robbins et al., 2016 for a review). Increasingly, studies utilize nontraditional stable isotope systems to gain further insights into the cycling of trace metals in the early oceans. This has proven especially useful for the first row of transition metals, except for monoisotopic elements like manganese (Mn) and Co. Early thermodynamic models were the basis of several inferences regarding how the emergent biosphere would have been affected by the availability of trace metals (e.g., Anbar and Knoll, 2002; Dupont et al., 2006, 2010). Yet a purely thermodynamic view, where metal speciation, concentration, and availability is estimated primarily based on the prevailing marine conditions (ferruginous, euxinic, oxic), has benefited from additional considerations such as how changes in volcanism have affected trace metal sourcing (e.g., Konhauser et al., 2009; Liu et al., 2021) and how oxygenation affected the flux of redox sensitive metals to the late Archean and early Paleoproterozoic oceans (e.g., Scott et al., 2008; Konhauser et al., 2011; Mänd et al., 2020).

## Molybdenum

While Mo is a key component of the widely used version of the metalloenzyme nitrogenase, and there has been significant interest in reconstructing its history in the early oceans (Fig. 4.7.1.2a) and the implications for nitrogen fixation and primary productivity (e.g., Anbar and Knoll, 2002; Glass et al., 2009; Zhang et al., 2014; Stüeken et al., 2015), we discuss it here with respect to its utility in tracking the rise of $O_2$ (e.g., Scott et al., 2008) and the expansion of euxinic environments which capture the seawater Mo isotopic signal (e.g., Asael et al., 2018). Molybdenum is sourced from the oceans through the oxidative weathering of terrestrial sulfide minerals. In the modern, well-oxygenated oceans, Mo is the most abundant transition metal (~104 nM) and displays a conservative profile where the concentration does not vary significantly with depth (e.g., Bruland et al., 2014). Yet in the Archean, given the lack of oxidative weathering under an anoxic atmosphere, it is expected that Mo abundances in seawater were exceedingly low and would have presented a potential limitation on nitrogen fixation (Anbar and Knoll, 2002). As Mo reacts with both organic matter and sulfides to increase burial fluxes, the record of reconstructing Mo abundances and variability through time has primarily been based on the analysis of black shale samples. In this regard, Anbar et al. (2007) examined ~2.5 Ga Mt. McRae black shale and attributed a transient Mo enrichment to a 'whiff' of $O_2$ prior to the GOE, while Scott et al. (2008) examined Mo in black shales to assess the Proterozoic onset and putative two-step structure of Earth's surface oxygenation. Subsequently, Stüeken et al. (2012) and Johnson et al. (2021) demonstrated a statistically significant increase in Mo concentrations in clastic marine sediments (i.e., black shales) at ~2.7 Gyr ago, attributing the increase in Mo fluxes to the biological weathering of sulfides on land and providing estimates for marine Mo concentration and $O_2$, respectively. Similarly, Mo enrichments in black shales have been interpreted to reflect oxidative weathering and shallow marine $O_2$ along continental margins ~2.6 to 2.5 Gyr ago (Kendall et al., 2010).

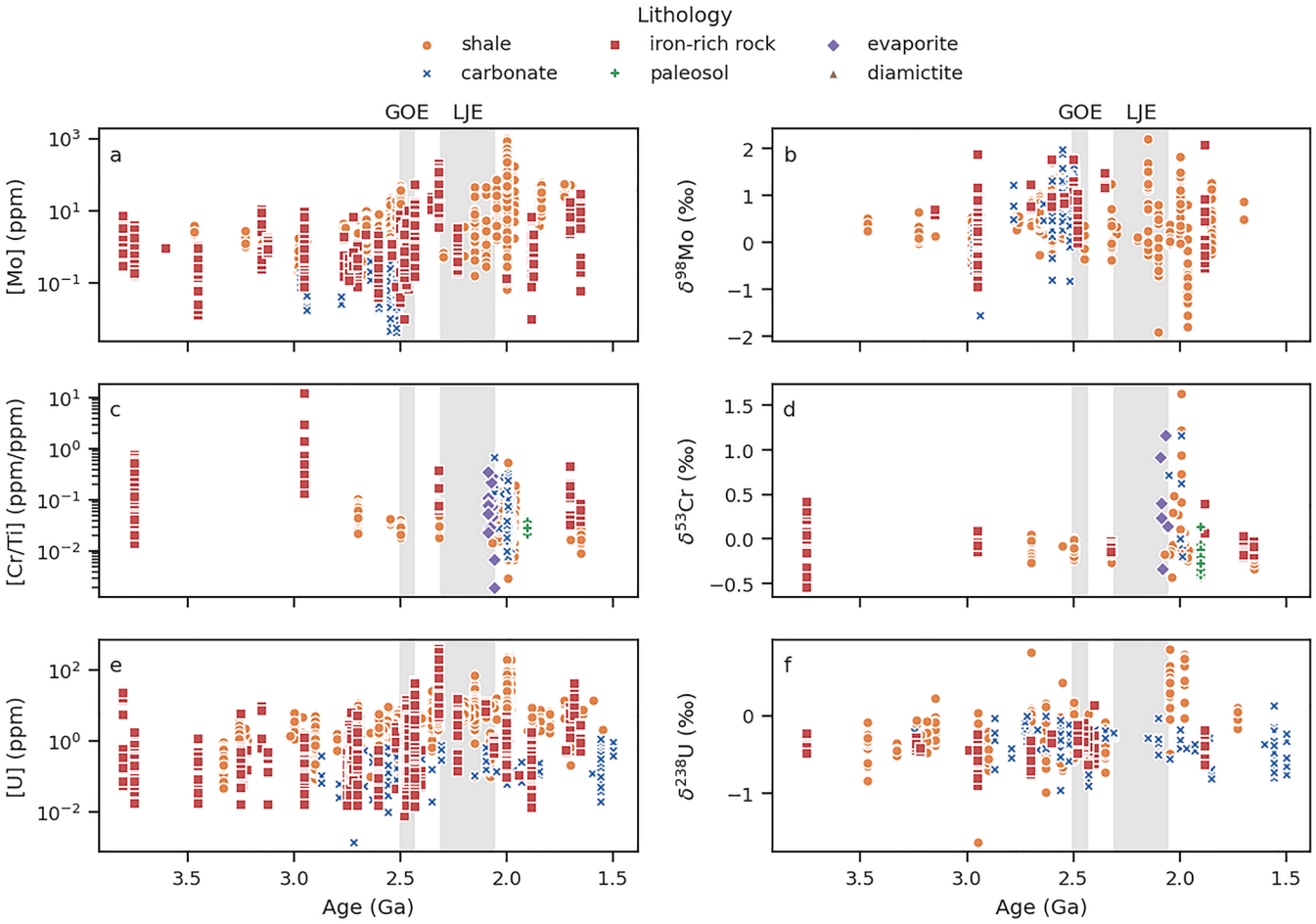


**FIGURE 4.7.1.2** Concentrations (a, c, e) and isotope ratios (b, d, f) of the redox-sensitive metals Mo (a, b), Cr (c, d), and U (e, f) in various sedimentary rock types through the Archean and Paleoproterozoic. Vertical gray bars represent the great oxidation event (GOE; Warke et al., 2020) and the Lomagundi-Jatuli carbon isotope excursion (LJE; Martin et al., 2013). Mo data comes from Luo et al. (2021) and the compilation of Mänd et al. (2021); Cr data from Frei et al. (2016) and the compilation of Mänd et al. (2022); and U data from the compilations of Partin et al. (2013a, b) and Chen et al. (2021).

Additional utility is found in the Mo isotope system (often reported as $\delta^{98/95}$Mo or $\delta^{98}$Mo) for reconstructing Archean to Proterozoic marine conditions (Fig. 4.7.1.2b). In euxinic settings, Mo is complexed by thiomolybdates and may be quantitatively removed given dissolved sulfide concentrations greater than 11 μM (e.g., Helz et al., 1996; Neubert et al., 2008). Under such conditions, the $\delta^{98}$Mo signal of open seawater may be captured. The Mo isotopic composition of the ocean is largely controlled by the adsorption of light Mo to Mn oxides, which drives the marine reservoir toward heavier values (e.g., Scott and Lyons, 2012; Kendall et al., 2017). To this end, light $\delta^{98}$Mo in the ~2.95 Ga Sinqeni Formation from South Africa are recorded in a succession with low Fe/Mn ratios. This implies that Mn oxides were present at that time, and by extension $O_2$, providing some of the earliest geochemical evidence for the activity of oxygenic photosynthesis (Planavsky et al., 2014a). Similarly, heavy $\delta^{98}$Mo values recorded in Archean shales and carbonates have been used to argue for the presence of environmental $O_2$, and thus oxygenic photosynthesis prior to the onset of the GOE (e.g., Duan et al., 2010; Czaja et al., 2012). Carbonate samples dated to 2.93 Ga further reveal significant heavy $\delta^{98}$Mo values, again pointing to the adsorption of light Mo onto Fe and Mn oxides, and presence of $O_2$ within the Mesoarchean water column (Thoby et al., 2019). Collectively, these Mo isotope results remain some of the oldest and most robust evidence for the onset of oxygenation in the Archean.

## Chromium

Chromium is a relatively common component in (ultra-)mafic igneous rocks, and hence it is more enriched in Archean rocks relative to Proterozoic rocks because of mantle cooling and a compositional shift to more

felsic igneous rocks (Liu et al., 2021). Chromium also has two oxidation states, +3 and + 6. Cr(III) is present in generally insoluble minerals such as chromite, and thus accumulates in soils (Oze et al., 2007). In the presence of Mn(IV) oxides (e.g., birnessite), the oxidation of Cr(III) leads to the solubilization and transport of Cr (VI) in the form of chromate, $CrO_4^{2-}$ (Fendorf, 1995). Additionally, in the absence of Mn(IV) oxides, Cr(III) may be solubilized by the complexation with organic ligands (D'Arcy et al., 2016). Collectively, these processes result in an authigenic marine cycle (Fig. 4.7.1.3). Accumulating in the oceans today mainly as dissolved chromate (Elderfield, 1970), Cr is sequestered most effectively by incorporation into anoxic or hypoxic sediments. Given the role of Mn(IV) in Cr weathering, modern Cr concentrations in shales still outstrip Proterozoic ones despite decreasing Cr input from the mantle (Reinhard et al., 2013).

More than concentrations (Fig. 4.7.1.2c), however, Cr isotope compositions (Fig. 4.7.1.2d) are commonly exploited for paleoenvironmental inferences because fractionation was thought to arise only during Cr(III) oxidation in the presence of Mn(IV) oxides in subaerial weathering settings, which, in turn, implies appreciable $O_2$ concentrations in the atmosphere (Frei et al., 2009). The first faint signs of oxic Cr cycling date back to roughly 3.7 Ga, where metasedimentary rocks from the Isua Supracrustal Belt in Greenland record some fractionated Cr (Fig. 4.7.1.2d). These data were interpreted to reflect minor amounts of reactive oxygen species formed during rock alteration, which can oxidize Mn (II) (Frei et al., 2016). Further signs of oxic Cr cycling are known from the 3.0 Ga Ijzermyn iron formation in South Africa (Crowe et al., 2013), being one of the archetypical "$O_2$ whiffs" of the late Archean. Following the GOE in the Paleoproterozoic, signs of oxic Cr cycling become more apparent, for example, in IF (Frei et al., 2009; Planavsky et al., 2014b), as well as shales and carbonates (e.g., Gilleaudeau et al., 2016; Mänd et al., 2022). However, several factors have emerged in recent years to complicate this narrative. First, the fractionated Cr isotopes in the 3.0 Ga Ijzermyn iron formation have been linked to recent weathering-related alteration of the original Cr isotopes (Albut et al., 2018), highlighting the pitfalls of assessing paleoredox in billions-of-years-old rocks using easily mobilized trace components. Similarly, work on paleosols has indicated that enriched Cr isotope signatures may be generated through the removal of isotopically light, reduced Cr(III) during alteration or pedogenesis (e.g., Babechuk et al., 2016). Moreover, the importance of detrital Cr solubilization in marine sediments has been reassessed by Miletto et al. (2021), with the implication that fractionated Cr need not derive solely from subaerial weathering, but that rapid Cr(III) oxidation in the marine realm may result in appreciable fractionations of >1‰. Finally, several mechanisms have been proposed through which Mn(IV) oxides can form in the absence of $O_2$—that is, biological or photochemical Mn oxidation (e.g., Daye et al., 2019; Liu et al., 2020), yet it remains unclear whether these alternative mechanisms can plausibly supply the required flux of Mn oxide to allow oxidized Cr species to form or persist in an anoxic environment (Planavsky et al., 2021). Alternative processes that may account for the heavy fractionated Cr isotopes have also been proposed, such as hydrocarbon migration (Qu et al., 2012), diagenetic redistribution (Frank et al., 2020), or the solubilization of reduced Cr by organic ligands (Saad et al., 2017). Nevertheless, the trend in Cr concentrations and isotope fractionation through Earth history remains consistent with our view of redox evolution based on other redox proxies.

## Uranium

Similar to Mo, U present in exhumed rocks as reduced phases (U(IV)) is mobilized in its oxidized version (U(VI)) as a uranyl carbonate complex and concentrates in $O_2$-rich oceans (Ku et al., 1977). Uranium may also be mobilized by organic ligands (e.g., Luo and Gu, 2009). It is most efficiently sequestered under anoxic or euxinic conditions as the reduced form (Anderson et al., 1989). Compilations of U in black shales and IF (Fig. 4.7.1.2e) show a strong coherence to the patterns observed in the Mo record (Partin et al., 2013a, 2013b), thus supporting the initial oxygenation of Earth's surface environments around the Archean–Proterozoic boundary. Based on a survey of U isotopes in geological samples and modern observations, Weyer et al. (2008) and Andersen et al. (2014), respectively, provided a framework through which U isotopes can be interpreted to provide evidence for oxidative weathering and water column oxygenation in the ancient oceans. In this regard, heavy $\delta^{238}U$ values (>+0.5‰) in ancient sediments (Fig. 4.7.1.2f) may be interpreted as reflecting both high seawater values and the full expression of fractionation during U reduction (Andersen et al., 2014). Archean values for $\delta^{238}U$ in IF, shales, and paleosols typically limited fractionation, but that variability increases at around 3.0 Ga, coinciding with the effects of oxygenic photosynthesis (Wang et al., 2018). Interestingly, it is not until almost 2.0 Ga that the first heavy $\delta^{238}U$ values are observed in sediments from the Zaonega Basin, indicating pervasive oxygenation in the wake of the Lomagundi-Jatuli Event (Fig. 4.7.1.2f; Mänd et al., 2020). Yet, aside from the above example, there is no overall change in the average $\delta^{238}U$ values coinciding with the GOE, possibly due to very low U residence times in seawater precluding the generation

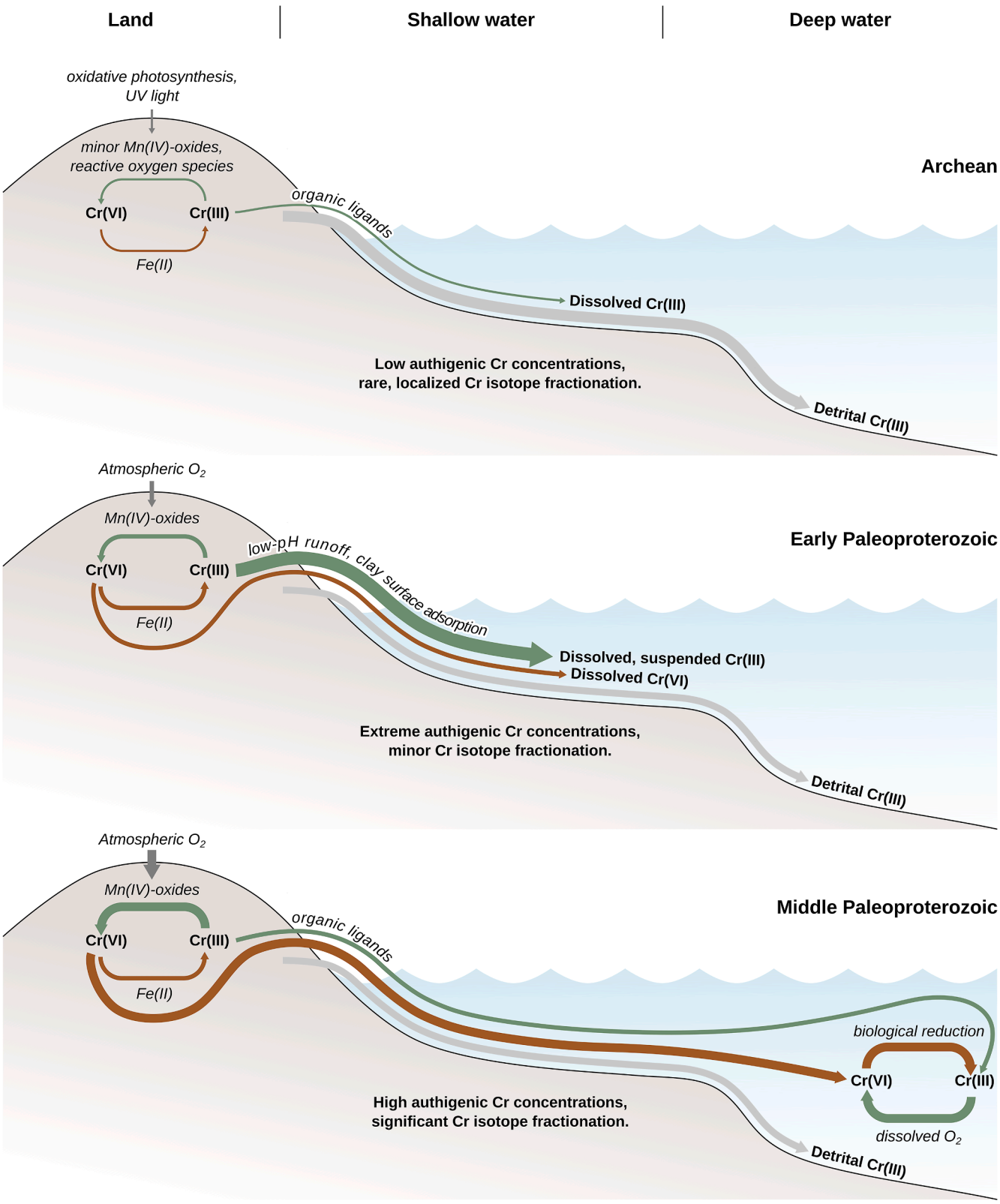


**FIGURE 4.7.1.3** Three modes of Cr cycling in Earths surface environments. In the Archean (top panel), high Cr concentrations in ultramafic rocks ensured a large detrital Cr(III) flux to sediments (Liu et al., 2021). Only very minor Cr isotope fractionation has been detected, possibly due to incipient oxygenic photosynthesis or photochemically produced reactive oxygen species (Frei et al., 2009, 2016). In the early Paleoproterozoic (middle panel), high Cr concentrations in shallow-water if have been linked to acid runoff due to pyrite oxidation under a newly oxygenated atmosphere (Konhauser et al., 2011; Hao et al., 2022). In the middle Paleoproterozoic, significant atmospheric $O_2$ ensured relatively high authigenic Cr concentrations in sediments and, for the first time, significant isotope fractionation (Mänd et al., 2022).

of significant fractionation or nonuniformity in the mechanisms governing U isotope fractionation in anoxic sediments (Chen et al., 2021). It is also possible that diagenetic effects may have played a role here; however, for black shales, diagenetic effects are expected to be relatively minor compared to carbonates as a result of their lower permeability (Lau et al., 2019).

## Cobalt and nickel

Both Co and Ni play key biochemical roles and have received attention for how potential changes in their availability through time may have affected the evolution of the biosphere. Cobalt, as the cofactor cobalamin, is essential for a number of metalloenyzmes (e.g., Marsh, 1999), while Ni sees heavy use in many prokaryotic metalloenyzmes necessary for carbon reduction and methane production (e.g., Hausinger, 1987), along with hydrogenases, dehydrogenases, and a version of super oxide dismutase (Ragsdale and Kumar, 1996; Dupont et al., 2008). We discuss Co and Ni here together, as they have somewhat similar geological histories, broadly decreasing from the Archean–Paleoproterozoic to modern (Konhauser et al., 2009, 2015; Swanner et al., 2014; Large et al., 2014) and are moderately correlated in the sedimentary pyrite record (Gregory et al., 2015).

Compilations of Co abundances (Fig. 4.7.1.3e) shown to date have largely been based on the sedimentary to early diagenetic pyrite record, shales, and IFs (Large et al., 2014; Gregory et al., 2015; Swanner et al., 2014). Overall, the Co compilations point to a general decline in Co abundances in marine systems from the Archean onwards. Against this overall fall in Co, however, statistically significant changes in the IF and euxinic shale records suggest expansion of the Co reservoir between 2.8 and 1.8 Ga, as reflected in mean Co/Ti or Co concentrations. This has been attributed to increased mantle plume activity and the circulation of hydrothermal fluids through ultramafic crust (Swanner et al., 2014). Implicit in this interpretation is that the decline in Co is associated with a decrease in hydrothermal activity and a change in the volcanic regime.

It has been proposed that a unidirectional decline in Ni concentrations at about 2.7 Ga preceded the onset of the GOE (Konhauser et al., 2009, 2015), and that this was attributable to declining mantle temperatures and the loss of komatiite eruptions and subsequent weathering. This hypothesis was derived based on the change in Ni/Fe ratios in IFs, backed up by a compilation of continental volcanics showing a concomitant decrease in Ni (Liu et al., 2021). The biological significance of declining seawater Ni is that methanogens starved and became marginalized to deeper water environments. This, in turn, facilitated the rise of cyanobacteria in shallow-water ecosystems. The Archean to Paleoproterozoic trend is mirrored in the pyrite record (Large et al., 2014; Gregory et al., 2015), although it shows a slight uptick in both the Neoproterozoic and Cenozoic (e.g., Gregory et al., 2015). The relative stabilization of Ni after 2.0 Ga may be the result of increased melting pressures, and the stabilization of basalt-andesite Ni concentrations, the combined effect of which prevented a further decline in Ni being sourced to the Earth's evolving oceans (Liu et al., 2021).

The application of Ni stable isotopes (Fig. 4.7.1.3f), primarily $\delta^{60/58}$Ni, is an emerging tool for reconstructing the Archean Ni cycle. Wasylenki et al. (2015) demonstrated that the adsorption of Ni to ferrihydrite, the likely precursor mineral phase to IFs (e.g., Konhauser et al., 2017), results in a predictable offset of +0.35‰ between the solid phase and solution. This decreases to +0.23% following aging to hematite and goethite, although these two offsets were within the uncertainty of one another. Further experimental results suggest that the isotopic composition of Ni in IFs should be robust against the effects of early diagenetic phase transitions (Wang and Wasylenki, 2017). While there are still relatively few studies of the Ni stable isotope system, they are beginning to yield novel insights into changes in the Archean to Paleoproterozoic Ni cycle. For instance, an increase in the $\delta^{60}$Ni composition recorded in diamictites coincident with the GOE has been interpreted to reflect the onset of sulfidic weathering (Wang et al., 2019). Those authors further suggested that this limited flux of Ni from the oxidative weathering of sulfides, following the decline associated with the loss of komatiite weathering and rise in $O_2$, would have been essential for supporting at least some methanogenesis and preventing the onset of a permanent glaciation.

Both Co and Ni represent bioessential elements whose geochemical cycling at the surface has been greatly impacted by long-term cooling in Earth's mantle, and as a result have likely declined since the Archean. While sinks have certainly changed, the fundamental shift in the source of Co and Ni to the oceans has exerted a strong first-order control on their temporal trends, reflecting the connection between Earth's mantle evolution and its surface processes.

## Zinc and copper

Zinc and Cu (Fig. 4.7.1.4) are largely sourced through the oxidative weathering of terrestrial sulfide minerals, and as such, they were likely to have been in lower concentrations in Archean seawater than the modern due to the lack of atmospheric $O_2$. As oxidative weathering became more prevalent following the rise of

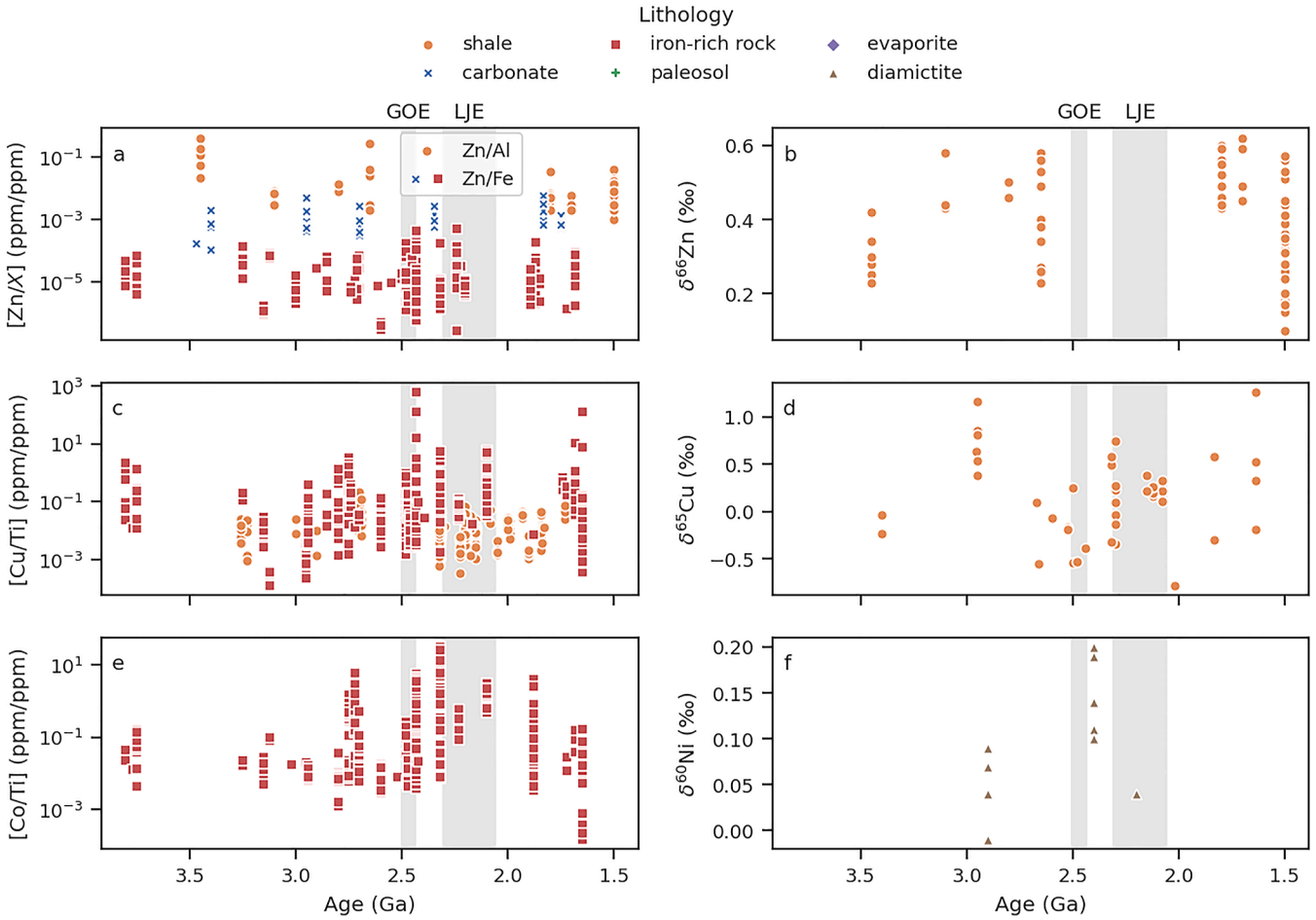


**FIGURE 4.7.1.4** Concentrations (a, c, e) and isotope ratios (b, d, f) of trace metals Zn (a, b), Cu (c, d), Co (e) and Ni (f) in various sedimentary rock types through the Archean and Paleoproterozoic. *Legend as on Fig. 4.7.1.3. Zn data comes from the compilations of Robbins et al. (2013), Liu et al. (2016), and Isson et al. (2018); Cu data from Chi Fru et al. (2016) and Ciscato et al. (2019); Co data from Swanner et al. (2014); and Ni data from Wang et al. (2019).*

atmospheric $O_2$ at ~2.5 Ga (Konhauser et al., 2011; Warke et al., 2020), the flux of sulfate and trace elements hosted in sulfides to the oceans would have increased. The increased flux of sulfate would be expected to increase the degree of bacterial sulfate reduction and drive the onset of euxinia in an otherwise dominantly anoxic ocean. Such a view led to the hypothesis that the early Proterozoic ocean would have been strongly euxinic (Canfield, 1998). Strongly euxinic conditions, in turn, would have led to the near quantitative sequestration of Cu and Zn in the expanded euxinic settings (Saito et al., 2003), thereby limiting their availability and strongly attenuating the marine reservoir at this time (e.g., Dupont et al., 2010). However, subsequent studies of the shale and IF records have indicated a far more static record of Zn and Cu through time (Fig. 4.7.1.4 a & c; Scott et al., 2013; Robbins et al., 2013; Chi Fru et al., 2016). Exceptions do arise, as an analysis of sedimentary to early diagenetic pyrite record indicates a transient increase in Zn at ~2.5 Ga followed by attenuated Proterozoic levels prior to a Phanerozoic increase. Copper seems to decrease from the Archean to a mid-Proterozoic low, before a slight rebound leading into a Neoproterozoic-to-Phanerozoic decline (Large et al., 2014).

One interesting possibility is that complexing by organic ligands can explain the muted temporal changes of Zn abundances observed in the IF record, as first suggested by Robbins et al. (2013). Geochemical models demonstrate that a nanomolar pool of a generic organic ligand could quickly dominate Zn speciation in simulated Archean seawater, thereby buffering the Zn reservoir against drawdown by increasing sulfide concentrations. Similarly, Stüeken (2020) demonstrated that organic ligands could have stabilized an increased hydrothermal flux of Cu to the Archean ocean and thereby mitigated the potential for a biological Cu limitation.

The emerging picture of an Archean to Proterozoic Zn and Cu reservoir that has been stable over geologically

long time scales, while somewhat surprisingly, highlights the need for an improved understanding of both marine trace metal speciation as well as how metal bioavailability has shifted over the last four billion years. To this end, a recent study demonstrated that ancestral lineages to modern cyanobacteria utilized both Cu and Zn to combat the redox stresses that emerged along with the rise of $O_2$ through their incorporation into the earliest form of a superoxide dismutase (*CuZnSOD*; Boden et al., 2021). The emergence of *CuZnSOD* likely occurred early, between 2.9 and 2.6 Ga (Boden et al., 2021), which may indicate either organically complexed Cu and Zn being bioavailable, or their utilization due to biologically intrinsic factors such as a lack of competition from other microbial lineages at this time. In either event, the early emergence of the *CuZnSOD* points to the availability of these elements in shallow Archean marine environments.

## Summary

First-order trends in trace metal abundances recorded in black shales, iron formations, carbonates, and sedimentary to early-diagenetic pyrite have led to key insights into the structure of Archean to Paleoproterozoic marine environments, the emergence of oxygenic photosynthesis and the subsequent oxygenation of Earth's surface environments. Metal cycling in the Archean occurred under dominantly anoxic conditions, with an atmosphere devoid of $O_2$ and oceans sourced by greater submarine hydrothermal fluxes that led to ferruginous conditions. By the Paleoproterozoic, the influence of atmospheric oxygenation and oxidative weathering of reduced crustal minerals then became an important factor, with greater fluxes of sulfate leading to euxinia in near-coastal settings. This resulted in an increased abundance of RSE and an increase in positively fractionated metal stable isotopes (e.g., U and Mo) that follows the onset of the GOE. The relatively stable records for Zn and Cu also hint at the possible influence of organic ligands in stabilizing marine metal abundances over geological timescales.

Further, advances in mass spectrometry have led to the utilization of a suite of transition metal stable isotope systematics that are continuing to yield novel insights into both Archean metal cycling and environmental conditions. These isotopic studies are being increasingly informed by a refined knowledge regarding modern marine metal cycles. The identification of mechanisms through which metal isotopes may be fractionated, such as the potential for ligand-induced solubilization, requires a reconsideration of the potential significance of isotopic signals and their relation to Archean conditions. Indeed, recent studies have begun to identify how oxidative weathering may affect the preservation of primary geochemical and isotopic signals, particularly in outcrop samples.

Future investigations will continue to rely on a diverse suite of trace metal and isotopic proxies to generate new information about Earth's early surface environments and biosphere. In addition, improving stratigraphic resolution and sampling density will not only provide short-term temporal trends that have previously gone unrecognized, but may also yield insights into the role of diagenesis (e.g., Albut et al., 2018) and trace element cycling (Alcott et al., 2022), thus potentially leading to new interpretations of paleomarine conditions from the trace metal record. This will allow for addressing critical questions such as: When did oxygenic photosynthesis first evolve? Which metabolisms were most prevalent in the Archean, and when did various metalloenzymes acquire metals? When did continents first emerge? And, how has the balance between metal sources and sinks evolved over Earth's history?

## References

Albut, G., Babechuk, M.G., Kleinhanns, I.C., Benger, M., Beukes, N.J., Steinhilber, B., Smith, A.J.B., Kruger, S.J., Schoenberg, R., 2018. Modern rather than Mesoarchaean oxidative weathering responsible for the heavy stable Cr isotopic signatures of the 2.95 Ga old Ijzermijn iron formation (South Africa). Geochim Cosmochim Ac 228, 157–189. https://doi.org/10.1016/j.gca.2018.02.034.

Alcott, L.J., Mills, B.J.W., Bekker, A., Poulton, S.W., 2022. Earth's Great Oxidation Event facilitated by the rise of sedimentary phosphorous recycling. Nat. Geosci. 15, 210–215. https://doi.org/10.1038/s41561-022-00906-5.

Anbar, A.D., 2008. Elements and evolution. Science 322, 1481–1483. https://doi.org/10.1126/science.1163100.

Anbar, A.D., Knoll, A.H., 2002. Proterozoic ocean chemistry and evolution: a bioinorganic bridge? Science 297, 1137–1142. https://doi.org/10.1126/science.1069651.

Anbar, A.D., Duan, Y., Lyons, T.W., Arnold, G.L., Kendall, B., Creaser, R.A., Kaufman, A.J., Gordon, G.W., Scott, C., Garvin, J., Buick, R., 2007. A whiff of oxygen before the Great oxidation event? Science 317, 1903–1906. https://doi.org/10.1126/science.1140325.

Andersen, M.B., Romaniello, S., Vance, D., Little, S.H., Herdman, R., Lyons, T.W., 2014. A modern framework for the interpretation of 238U/235U in studies of ancient ocean redox. Earth Planet Sc Lett 400, 184–194. https://doi.org/10.1016/j.epsl.2014.05.051.

Anderson, R.F., Fleisher, M.Q., LeHuray, A.P., 1989. Concentration, oxidation state, and particulate flux of uranium in the Black Sea. Geochim Cosmochim Ac 53, 2215–2224. https://doi.org/10.1016/0016-7037(89)90345-1.

Asael, D., Rouxel, O.J., Poulton, S.W., Lyons, T.W., Bekker, A., 2018. Molybdenum record from black shales indicates oscillating atmospheric oxygen levels in the early Paleoproterozoic. Am. J. Sci. 318, 275–299. https://doi.org/10.2475/03.2018.01.

Babechuk, M.G., Kleinhanns, I.C., Schoenberg, R., 2016. Chromium geochemistry of the ca. 1.85 Ga Flin Flon paleosol. Geobiology 15, 30–50. https://doi.org/10.1111/gbi.12203.

Bau, M., Möller, P., 1993. Rare earth element systematics of the chemically precipitated component in Early Precambrian iron formations and the evolution of the terrestrial atmosphere-hydrosphere-lithosphere system. Geochim Cosmochim Ac 57, 2239–2249. https://doi.org/10.1016/0016-7037(93)90566-f.

Bekker, A., Planavsky, N.J., Krapez, B., Rasmussen, B., Hofmann, A., Slack, J.F., Rouxel, O.J., Konhauser, K.O., 2014. Iron formations: their origins and implications for ancient seawater chemistry. In: Treatise on Geochemistry. Elsevier, pp. 561–628. https://doi.org/10.1016/b978-0-08-095975-7.00719-1.

Bruland, K.W., Middag, R., Lohan, M.C., 2014. Controls of trace metals in seawater. In: Holland, H.D., Turekian, K. (Eds.), Treatise on Geochemistry, pp. 19–51. https://doi.org/10.1016/b978-0-08-095975-7.00602-1.

Boden, J.S., Konhauser, K.O., Robbins, L.J., Sánchez-Baracaldo, P., 2021. Timing the evolution of antioxidant enzymes in cyanobacteria. Nat. Commun. 12, 4742. https://doi.org/10.1038/s41467-021-24396-y.

Catling, D.C., Zahnle, K.J., 2020. The Archean atmosphere. Sci. Adv. 6, eaax1420. https://doi.org/10.1126/sciadv.aax1420.

Canfield, D., 1998. A new model for Proterozoic ocean chemistry. Nature 396, 450–453.

Chi Fru, E., Rodríguez, N.P., Partin, C.A., Lalonde, S.V., Andersson, P. S., Weiss, D.J., Albani, A.E., Rodushkin, I., Konhauser, K.O., 2016. Cu isotopes in marine black shales record the Great Oxidation Event. Proc National Acad Sci 113, 4941–4946. https://doi.org/10.1073/pnas.1523544113.

Chen, X., Tissot, F.L.H., Jansen, M.F., Bekker, A., Liu, C.X., Nie, N.X., Halverson, G.P., Veizer, J., Dauphas, N., 2021. The uranium isotopic record of shales and carbonates through geologic time. Geochim Cosmochim Ac 300, 164–191. https://doi.org/10.1016/j.gca.2021.01.040.

Ciscato, E.R., Bontognali, T.R.R., Poulton, S.W., Vance, D., 2019. Copper and its isotopes in organic-rich sediments: from the modern Peru margin to archean shales. Geosciences 9, 325. https://doi.org/10.3390/geosciences9080325.

Cloud, P., 1973. Paleoecological significance of the banded iron-formation. Econ. Geol. 68, 1135–1143.

Crowe, S.A., Døssing, L.N., Beukes, N.J., Bau, M., Kruger, S.J., Frei, R., Canfield, D.E., 2013. Atmospheric oxygenation three billion years ago. Nature 501, 535–538. https://doi.org/10.1038/nature12426.

Czaja, A.D., Johnson, C.M., Roden, E.E., Beard, B.L., Voegelin, A.R., Nägler, T.F., Beukes, N.J., Wille, M., 2012. Evidence for free oxygen in the Neoarchean ocean based on coupled iron–molybdenum isotope fractionation. Geochim Cosmochim Ac 86, 118–137. https://doi.org/10.1016/j.gca.2012.03.007.

Czaja, A.D., Johnson, C.M., Beard, B.L., Roden, E.E., Li, W., Moorbath, S., 2013. Biological Fe oxidation controlled deposition of banded iron formation in the ca. 3370 Ma Isua Supracrustal Belt (West Greenland). Earth Planet Sci. Lett. 363, 192–203. https://doi.org/10.1016/j.epsl.2012.12.025.

D'Arcy, J., Babechuk, M.G., Døssing, L.N., Gaucher, C., Frei, R., 2016. Processes controlling the chromium isotopic composition of river water: constraints from basaltic river catchments. Geochim Cosmochim Ac 186, 296–315. https://doi.org/10.1016/j.gca.2016.04.027.

Daye, M., Klepac-Ceraj, V., Pajusalu, M., Rowland, S., Farrell-Sherman, A., Beukes, N., Tamura, N., Fournier, G., Bosak, T., 2019. Light-driven anaerobic microbial oxidation of manganese. Nature 576, 311–314. https://doi.org/10.1038/s41586-019-1804-0.

Duan, Y., Anbar, A.D., Arnold, G.L., Lyons, T.W., Gordon, G.W., Kendall, B., 2010. Molybdenum isotope evidence for mild environmental oxygenation before the Great Oxidation Event. Geochim Cosmochim Ac 74, 6655–6668. https://doi.org/10.1016/j.gca.2010.08.035.

Dupont, C., Yang, S., Palenik, B., Bourne, P., 2006. Modern proteomes contain putative imprints of ancient shifts in trace metal geochemistry. Proc. Natl. Acad. Sci. 103, 17822–17827.

Dupont, C.L., Neupane, K., Shearer, J., Palenik, B., 2008. Diversity, function and evolution of genes coding for putative Ni-containing superoxide dismutases. Environ. Microbiol. 10, 1831–1843. https://doi.org/10.1111/j.1462-2920.2008.01604.x.

Dupont, C., Butcher, A., Valas, R., Bourne, P., Caetano-Anollés, G., 2010. History of biological metal utilization inferred through phylogenomic analysis of protein structures. Proc National Acad Sci 107, 10567–10572. https://doi.org/10.1073/pnas.0912491107.

Elderfield, H., 1970. Chromium speciation in sea water. Earth Planet Sc Lett 9, 10–16. https://doi.org/10.1016/0012-821x(70)90017-8.

Fendorf, S., 1995. Surface reactions of chromium in soils and waters. Geoderma 67 (55), 71. https://doi.org/10.1016/0016-7061(94)00062-f.

Frank, A.B., Klaebe, R.M., Löhr, S., Xu, L., Frei, R., 2020. Chromium isotope composition of organic-rich marine sediments and their mineral phases and implications for using black shales as a paleoredox archive. Geochim Cosmochim Acta 270, 338–359. https://doi.org/10.1016/j.gca.2019.11.035.

Frei, R., Gaucher, C., Poulton, S.W., Canfield, D.E., 2009. Fluctuations in Precambrian atmospheric oxygenation recorded by chromium isotopes. Nature 461, 250–253. https://doi.org/10.1038/nature08266.

Frei, R., Crowe, S.A., Bau, M., Polat, A., Fowle, D.A., 2016. Oxidative elemental cycling under the low O2 Eoarchean atmosphere. Sci. Rep. 6, 21058. https://doi.org/10.1038/srep21058.

Gilleaudeau, G.J., Frei, R., Kaufman, A.J., Kah, L.C., Azmy, K., Bartley, J.K., Chernyavskiy, P., Knoll, A.H., 2016. Oxygenation of the mid-Proterozoic atmosphere: clues from chromium isotopes in carbonates. Geochem Perspectives Lett 178, 187. https://doi.org/10.7185/geochemlet.1618.

Glass, J.B., Wolfe-Simon, F., Anbar, A.D., 2009. Coevolution of metal availability and nitrogen assimilation in cyanobacteria and algae. Geobiology 7, 100–123. https://doi.org/10.1111/j.1472-4669.2009.00190.x.

Gregory, D.D., Large, R.R., Halpin, J.A., Baturina, E.L., Lyons, T.W., Wu, S., Danyushevsky, L.V., Sack, P.J., Chappaz, A., Maslennikov, V., Bull, S.W., 2015. Trace element content of sedimentary pyrite in black shales. Econ. Geol. 110, 1389–1410. https://doi.org/10.2113/econgeo.110.6.1389.

Hao, W., Chen, N., Sun, W., Mänd, K., Kirsimäe, K., Teitler, Y., Somelar, P., Robbins, L.J., Babechuk, M.G., Planavsky, N.J., Alessi, D.S., Konhauser, K.O., 2022. Binding and transport of Cr (III) by clay minerals during the Great oxidation event. Earth Planet Sc Lett 584, 117503. https://doi.org/10.1016/j.epsl.2022.117503.

Hausinger, R.P., 1987. Nickel utilization by microorganisms. Microbiol. Rev. 51, 22–42. https://doi.org/10.1128/mr.51.1.22-42.1987.

Hawkesworth, C.J., Cawood, P.A., Dhuime, B., Kemp, T.I.S., 2017. Earth's continental lithosphere through time. Annu. Rev. Earth Planet. Sci. 45, 169–198. https://doi.org/10.1146/annurev-earth-063016-020525.

Helz, G.R., Miller, C.V., Charnock, J.M., Mosselmans, J.F.W., Pattrick, R. A.D., Garner, C.D., Vaughan, D.J., 1996. Mechanism of molybdenum removal from the sea and its concentration in black shales: EXAFS evidence. Geochim Cosmochim Ac 60, 3631–3642. https://doi.org/10.1016/0016-7037(96)00195-0.

Isson, T.T., Love, G.D., Dupont, C.L., Reinhard, C.T., Zumberge, A.J., Asael, D., Gueguen, B., McCrow, J., Gill, B.C., Owens, J., Rainbird, R.H., Rooney, A.D., Zhao, M.-Y., Stueeken, E.E., Konhauser, K.O., John, S.G., Lyons, T.W., Planavsky, N.J., 2018. Tracking the rise of eukaryotes to ecological dominance with zinc isotopes. Geobiology 16, 341–352. https://doi.org/10.1111/gbi.12289.

Johnson, A.C., Ostrander, C.M., Romaniello, S.J., Reinhard, C.T., Greaney, A.T., Lyons, T.W., Anbar, A.D., 2021. Reconciling evidence of oxidative weathering and atmospheric anoxia on Archean Earth. Sci. Adv. 7, eabj0108. https://doi.org/10.1126/sciadv.abj0108.

Johnson, B.W., Wing, B.A., 2020. Limited Archaean continental emergence reflected in an early Archaean 18O-enriched ocean. Nat. Geosci. 13, 243–248. https://doi.org/10.1038/s41561-020-0538-9.

Kappler, A., Pasquero, C., Konhauser, K.O., Newman, D.K., 2005. Deposition of banded iron formations by anoxygenic phototrophic Fe(II)-oxidizing bacteria. Geology 33 (1), 865–868. https://doi.org/10.1130/g21658.1.

Kendall, B., Reinhard, C.T., Lyons, T.W., Kaufman, A.J., Poulton, S.W., Anbar, A.D., 2010. Pervasive oxygenation along late Archaean ocean margins. Nat. Geosci. 3, 647–652. https://doi.org/10.1038/ngeo942.

Kendall, B., Gordon, G.W., Poulton, S.W., Anbar, A.D., 2011. Molybdenum isotope constraints on the extent of late Paleoproterozoic ocean euxinia. Earth Planet Sc Lett 307, 450–460. https://doi.org/10.1016/j.epsl.2011.05.019.

Kendall, B., Dahl, T.W., Anbar, A.D., 2017. The stable isotope geochemistry of molybdenum. Rev Mineralogy Geochem 82, 683–732. https://doi.org/10.2138/rmg.2017.82.16.

Krissansen-Totton, J., Arney, G.N., Catling, D.C., 2018. Constraining the climate and ocean pH of the early Earth with a geological carbon cycle model. Proc National Acad Sci 115, 4105–4110. https://doi.org/10.1073/pnas.1721296115.

Konhauser, K.O., Hamade, T., Raiswell, R., Morris, R., Ferris, F., Southam, G., Canfield, D., 2002. Could bacteria have formed the Precambrian banded iron formations? Geology 30, 1079–1082. https://doi.org/10.1130/0091-7613(2002)030<1079:cbhftp>2.0.co;2.

Konhauser, K.O., Pecoits, E., Lalonde, S.V., Papineau, D., Nisbet, E.G., Barley, M.E., Arndt, N.T., Zahnle, K., Kamber, B.S., 2009. Oceanic nickel depletion and a methanogen famine before the Great Oxidation Event. Nature 458, 750–753. https://doi.org/10.1038/nature07858.

Konhauser, K.O., Lalonde, S.V., Planavsky, N.J., Pecoits, E., Lyons, T.W., Mojzsis, S.J., Rouxel, O.J., Barley, M.E., Rosière, C., Fralick, P.W., Kump, L.R., Bekker, A., 2011. Aerobic bacterial pyrite oxidation and acid rock drainage during the Great Oxidation Event. Nature 478, 369–373. https://doi.org/10.1038/nature10511.

Konhauser, K.O., Robbins, L.J., Pecoits, E., Peacock, C., Kappler, A., Lalonde, S.V., 2015. The archean nickel famine Revisited. Astrobiology 15, 804–815. https://doi.org/10.1089/ast.2015.1301.

Konhauser, K.O., Planavsky, N.J., Hardisty, D.S., Robbins, L.J., Warchola, T.J., Haugaard, R., Lalonde, S.V., Partin, C.A., Oonk, P. B.H., Tsikos, H., Lyons, T.W., Bekker, A., Johnson, C.M., 2017. Iron formations: a global record of Neoarchaean to Palaeoproterozoic environmental history. Earth Sci. Rev. 172, 140–177. https://doi.org/10.1016/j.earscirev.2017.06.012.

Ku, T.-L., Knauss, K.G., Mathieu, G.G., 1977. Uranium in open ocean: concentration and isotopic composition. Deep Sea Res. 24, 1005–1017. https://doi.org/10.1016/0146-6291(77)90571-9.

Large, R.R., Halpin, J.A., Danyushevsky, L.V., Maslennikov, V.V., Bull, S.W., Long, J.A., Gregory, D.D., Lounejeva, E., Lyons, T.W., Sack, P.J., McGoldrick, P.J., Calver, C.R., 2014. Trace element content of sedimentary pyrite as a new proxy for deep-time ocean-atmosphere evolution. Earth Planet Sc Lett 389, 209–220. https://doi.org/10.1016/j.epsl.2013.12.020.

Lau, K.V., Romaniello, S.J., Zhang, F., 2019. The Uranium Isotope Paleoredox Proxy, Elements in Geochemical Tracers in Earth System Science. Cambridge University Press, Cambridge, United Kingdom. https://doi.org/10.1017/9781108584142.

Li, Y., Sutherland, B.R., Gingras, M.K., Owttrim, G.W., Konhauser, K. O., 2021. A novel approach to investigate the deposition of (bio) chemical sediments: the sedimentation velocity of cyanobacteria-ferrihydrite aggregates. J. Sed. Res 91, 390–398. https://doi.org/10.2110/jsr.2020.114.

Liu, H., Konhauser, K.O., Robbins, L.J., Sun, W., 2021. Global continental volcanism controlled the evolution of the oceanic nickel reservoir. Earth Planet Sc Lett 572, 117116. https://doi.org/10.1016/j.epsl.2021.117116.

Liu, W., Hao, J., Elzinga, E.J., Piotrowiak, P., Nanda, V., Yee, N., Falkowski, P.G., 2020. Anoxic photogeochemical oxidation of manganese carbonate yields manganese oxide. Proc National Acad Sci 117, 22698–22704. https://doi.org/10.1073/pnas.2002175117.

Liu, X.M., Kah, L.C., Knoll, A.H., Cui, H., Kaufman, A.J., Shahar, A., Hazen, R.M., 2016. Tracing Earth's O2 evolution using Zn/Fe ratios in marine carbonates. Geochem Perspectives Lett 2, 24–34. https://doi.org/10.7185/geochemlet.1603.

Luo, J., Long, X., Bowyer, F.T., Mills, B.J.W., Li, J., Xiong, Y., Zhu, X., Zhang, K., Poulton, S.W., 2021. Pulsed oxygenation events drove progressive oxygenation of the early Mesoproterozoic ocean. Earth Planet Sc Lett 559, 116754. https://doi.org/10.1016/j.epsl.2021.116754.

Luo, W., Gu, B., 2009. Dissolution and Mobilization of uranium in a reduced sediment by natural Humic Substances under anaerobic conditions. Environ. Sci. Technol. 43, 152–156. https://doi.org/10.1021/es8013979.

Mänd, K., Lalonde, S.V., Robbins, L.J., Thoby, M., Paiste, K., Kreitsmann, T., Paiste, P., Reinhard, C.T., Romashkin, A.E., Planavsky, N.J., Kirsimäe, K., Lepland, A., Konhauser, K.O., 2020. Palaeoproterozoic oxygenated oceans following the Lomagundi–Jatuli event. Nat. Geosci. 13, 302–306. https://doi.org/10.1038/s41561-020-0558-5.

Mänd, K., Robbins, L.J., Planavsky, N.J., Bekker, A., Konhauser, K., 2021. Iron Formations as Palaeoenvironmental Archives, Geochemical Tracers in Earth System Science. Cambridge University Press. https://doi.org/10.1017/9781108993791.

Mänd, K., Planavsky, N.J., Porter, S.M., Robbins, L.J., Wang, C., Kreitsmann, T., Paiste, K., Paiste, P., Romashkin, A.E., Deines, Y. E., Kirsimäe, K., Lepland, A., Konhauser, K.O., 2022. Chromium evidence for protracted oxygenation during the Paleoproterozoic. Earth Planet Sc Lett 584, 117501. https://doi.org/10.1016/j.epsl.2022.117501.

Marsh, E.N.G., 1999. Coenzyme B12 (cobalamin)-dependent enzymes. Essays Biochem. 34, 139–154.

Martin, A.P., Condon, D.J., Prave, A.R., Lepland, A., 2013. A review of temporal constraints for the Palaeoproterozoic large, positive carbonate carbon isotope excursion (the Lomagundi–Jatuli Event). Earth Sci. Rev. 127, 242–261. https://doi.org/10.1016/j.earscirev.2013.10.006.

Miletto, M., Wang, X., Planavsky, N.J., Luther, G.W., Lyons, T.W., Tebo, B.M., 2021. Marine microbial Mn(II) oxidation mediates Cr (III) oxidation and isotope fractionation. Geochim Cosmochim Ac 297, 101–119. https://doi.org/10.1016/j.gca.2021.01.008.

Muhling, J.R., Rasmussen, B., 2020. Widespread deposition of Greenalite to form banded iron formations before the Great oxidation event. Precambr. Res. 105619. https://doi.org/10.1016/j.precamres.2020.105619.

Neubert, N., Nägler, T.F., Böttcher, M.E., 2008. Sulfidity controls molybdenum isotope fractionation into euxinic sediments: evidence from the modern Black Sea. Geology 36 (1), 775–778. https://doi.org/10.1130/g24959a.1.

Oze, C., Bird, D., Fendorf, S., 2007. Genesis of hexavalent chromium from natural sources in soil and groundwater. Proc. Natl. Acad. Sci. 104, 6544–6549.

Partin, C.A., Bekker, A., Planavsky, N.J., Scott, C.T., Gill, B.C., Li, C., Podkovyrov, V., Maslov, A., Konhauser, K.O., Lalonde, S.V., Love, G.D., Poulton, S.W., Lyons, T.W., 2013a. Large-scale fluctuations in Precambrian atmospheric and oceanic oxygen levels from

the record of U in shales. Earth Planet Sc Lett 369–370, 284–293. https://doi.org/10.1016/j.epsl.2013.03.031.

Partin, C.A., Lalonde, S.V., Planavsky, N.J., Bekker, A., Rouxel, O.J., Lyons, T.W., Konhauser, K.O., 2013b. Uranium in iron formations and the rise of atmospheric oxygen. Chem. Geol. 362, 82–90. https://doi.org/10.1016/j.chemgeo.2013.09.005.

Planavsky, N.J., McGoldrick, P., Scott, C.T., Li, C., Reinhard, C.T., Kelly, A.E., Chu, X., Bekker, A., Love, G.D., Lyons, T.W., 2011. Widespread iron-rich conditions in the mid-Proterozoic ocean. Nature 477, 448–451. https://doi.org/10.1038/nature10327.

Planavsky, N.J., Asael, D., Hofmann, A., Reinhard, C.T., Lalonde, S.V., Knudsen, A., Wang, X., Ossa, F.O., Pecoits, E., Smith, A.J.B., Beukes, N.J., Bekker, A., Johnson, T.M., Konhauser, K.O., Lyons, T.W., Rouxel, O.J., 2014a. Evidence for oxygenic photosynthesis half a billion years before the Great Oxidation Event. Nat. Geosci. 7, 283–286. https://doi.org/10.1038/ngeo2122.

Planavsky, N.J., Reinhard, C.T., Wang, X., Thomson, D., McGoldrick, P., Rainbird, R.H., Johnson, T., Fischer, W.W., Lyons, T.W., 2014b. Low Mid-Proterozoic atmospheric oxygen levels and the delayed rise of animals. Science 346, 635–638. https://doi.org/10.1126/science.1258410.

Planavsky, N.J., Crowe, S.A., Fakhraee, M., Beaty, B., Reinhard, C.T., Mills, B.J.W., Holstege, C., Konhauser, K.O., 2021. Evolution of the structure and impact of Earth's biosphere. Nat. Rev. Earth Environ. 2, 123–139. https://doi.org/10.1038/s43017-020-00116-w.

Poulton, S.W., Canfield, D.E., 2011. Ferruginous conditions: a dominant Feature of the ocean through Earth's history. Elements 7, 107–112. https://doi.org/10.2113/gselements.7.2.107.

Qu, Y., Črne, A.E., Lepland, A., van Zuilen, M.A., 2012. Methanotrophy in a Paleoproterozoic oil field ecosystem, Zaonega formation, Karelia, Russia. Geobiology 10, 467–478. https://doi.org/10.1111/gbi.12007.

Ragsdale, S.W., Kumar, M., 1996. Nickel-Containing carbon Monoxide Dehydrogenase/Acetyl-CoA Synthase. Chem Rev 96, 2515–2540. https://doi.org/10.1021/cr950058+.

Rasmussen, B., Muhling, J.R., Krapež, B., 2021. Greenalite and its role in the genesis of early Precambrian iron formations – a review. Earth Sci. Rev. 217, 103613. https://doi.org/10.1016/j.earscirev.2021.103613.

Reinhard, C.T., Planavsky, N.J., Robbins, L.J., Partin, C.A., Gill, B.C., Lalonde, S.V., Bekker, A., Konhauser, K.O., Lyons, T.W., 2013. Proterozoic ocean redox and biogeochemical stasis. Proc National Acad Sci 110, 5357–5362. https://doi.org/10.1073/pnas.1208622110.

Robbins, L.J., Lalonde, S.V., Saito, M.A., Planavsky, N.J., Mloszewska, A.M., Pecoits, E., Scott, C., Dupont, C.L., Kappler, A., Konhauser, K.O., 2013. Authigenic iron oxide proxies for marine zinc over geological time and implications for eukaryotic metallome evolution. Geobiology 11, 295–306. https://doi.org/10.1111/gbi.12036.

Robbins, L.J., Lalonde, S.V., Planavsky, N.J., Partin, C.A., Reinhard, C.T., Kendall, B., Scott, C., Hardisty, D.S., Gill, B.C., Alessi, D.S., Dupont, C.L., Saito, M.A., Crowe, S.A., Poulton, S.W., Bekker, A., Lyons, T.W., Konhauser, K.O., 2016. Trace elements at the intersection of marine biological and geochemical evolution. Earth Sci. Rev. 163, 323–348. https://doi.org/10.1016/j.earscirev.2016.10.013.

Saad, E.M., Wang, X., Planavsky, N.J., Reinhard, C.T., Tang, Y., 2017. Redox-independent chromium isotope fractionation induced by ligand-promoted dissolution. Nat. Commun. 8, 1–10. https://doi.org/10.1038/s41467-017-01694-y.

Saito, M.A., Sigman, D., Morel, F., 2003. The bioinorganic chemistry of the ancient ocean: the co-evolution of cyanobacterial metal requirements and biogeochemical cycles at the Archean-Proterozoic boundary? Inorg. Chim. Acta. 356, 308–318. https://doi.org/10.1016/s0020-1693(03)00442-0.

Scott, C., Lyons, T.W., 2012. Contrasting molybdenum cycling and isotopic properties in euxinic versus non-euxinic sediments and sedimentary rocks: Refining the paleoproxies. Chem. Geol. 324, 19–27. https://doi.org/10.1016/j.chemgeo.2012.05.012.

Scott, C., Lyons, T.W., Bekker, A., Shen, Y., Poulton, S.W., Chu, X., Anbar, A.D., 2008. Tracing the stepwise oxygenation of the Proterozoic ocean. Nature 452, 456–459. https://doi.org/10.1038/nature06811.

Scott, C., Planavsky, N.J., Dupont, C.L., Kendall, B., Gill, B.C., Robbins, L.J., Husband, K.F., Arnold, G.L., Wing, B.A., Poulton, S.W., Bekker, A., Anbar, A.D., Konhauser, K.O., Lyons, T.W., 2013. Bioavailability of zinc in marine systems through time. Nat. Geosci. 6, 125–128. https://doi.org/10.1038/ngeo1679.

Smith, A.J.B., Beukes, N.J., Gutzmer, J., Czaja, A.D., Johnson, C.M., Nhleko, N., 2017. Oncoidal granular iron formation in the Mesoarchaean Pongola Supergroup, southern Africa: Textural and geochemical evidence for biological activity during iron deposition. Geobiology 15, 731–749. https://doi.org/10.1111/gbi.12248.

Smith, A.J.B., Beukes, N.J., Gutzmer, J., Johnson, C.M., Czaja, A.D., Nhleko, N., Beer, F. de, Hoffman, J.W., Awramik, S.M., 2020. Life on a Mesoarchean marine shelf – insights from the world's oldest known granular iron formation. Sci. Rep. 10, 10519. https://doi.org/10.1038/s41598-020-66805-0.

Stüeken, E.E., 2020. Hydrothermal vents and organic ligands sustained the Precambrian copper budget. Geochem Perspectives Lett 12–16. https://doi.org/10.7185/geochemlet.2037.

Stüeken, E.E., Catling, D.C., Buick, R., 2012. Contributions to late Archaean sulphur cycling by life on land. Nat. Geosci. 5, 722–725. https://doi.org/10.1038/ngeo1585.

Stüeken, E.E., Buick, R., Guy, B.M., Koehler, M.C., 2015. Isotopic evidence for biological nitrogen fixation by molybdenum-nitrogenase from 3.2 Gyr. Nature 520, 666–669. https://doi.org/10.1038/nature14180.

Swanner, E.D., Planavsky, N.J., Lalonde, S.V., Robbins, L.J., Bekker, A., Rouxel, O.J., Saito, M.A., Kappler, A., Mojzsis, S.J., Konhauser, K.O., 2014. Cobalt and marine redox evolution. Earth Planet Sc Lett 390, 253–263. https://doi.org/10.1016/j.epsl.2014.01.001.

Thoby, M., Konhauser, K.O., Fralick, P.W., Altermann, W., Visscher, P.T., Lalonde, S.V., 2019. Global importance of oxic molybdenum sinks prior to 2.6 Ga revealed by the Mo isotope composition of Precambrian. Geology 47, 559–562. https://doi.org/10.1130/g45706.1.

Tribovillard, N., Algeo, T.J., Lyons, T., Riboulleau, A., 2006. Trace metals as paleoredox and paleoproductivity proxies: an update. Chem. Geol. 232 (12), 32. https://doi.org/10.1016/j.chemgeo.2006.02.012.

Warke, M.R., Rocco, T.D., Zerkle, A.L., Lepland, A., Prave, A.R., Martin, A.P., Ueno, Y., Condon, D.J., Claire, M.W., 2020. The Great oxidation event preceded a Paleoproterozoic "snowball earth." Proc National Acad Sci 117, 13314–13320. https://doi.org/10.1073/pnas.2003090117.

Wang, S.-J., Wasylenki, L.E., 2017. Experimental constraints on reconstruction of Archean seawater Ni isotopic composition from banded iron formations. Geochim Cosmochim Ac 206, 137–150. https://doi.org/10.1016/j.gca.2017.02.023.

Wang, S.-J., Rudnick, R.L., Gaschnig, R.M., Wang, H., Wasylenki, L.E., 2019. Methanogenesis sustained by sulfide weathering during the Great oxidation event. Nat. Geosci. 361 (1), 6. https://doi.org/10.1038/s41561-019-0320-z.

Wang, X., Planavsky, N.J., Hofmann, A., Saupe, E.E., Corte, B.P.D., Philippot, P., LaLonde, S.V., Jemison, N.E., Zou, H., Ossa, F.O., Rybacki, K., Alfimova, N., Larson, M.J., Tsikos, H., Fralick, P.W., Johnson, T.M., Knudsen, A.C., Reinhard, C.T., Konhauser, K.O., 2018. A Mesoarchean shift in uranium isotope systematics.

Geochim Cosmochim Ac 1, 36. https://doi.org/10.1016/j.gca.2018.07.024.

Wasylenki, L.E., Howe, H.D., Spivak-Birndorf, L.J., Bish, D.L., 2015. Ni isotope fractionation during sorption to ferrihydrite: implications for Ni in banded iron formations. Chem. Geol. 400, 56–64. https://doi.org/10.1016/j.chemgeo.2015.02.007.

Weyer, S., Anbar, A.D., Gerdes, A., Gordon, G.W., Algeo, T.J., Boyle, E. A., 2008. Natural fractionation of 238U/235U. Geochim. Cosmochim. Acta 72, 345–359. https://doi.org/10.1016/j.gca.2007.11.012.

Zhang, X., Sigman, D.M., Morel, F.M.M., Kraepiel, A.M.L., 2014. Nitrogen isotope fractionation by alternative nitrogenases and past ocean anoxia. Proc National Acad Sci 111, 4782–4787. https://doi.org/10.1073/pnas.1402976111.